

**The Long Wavelength Array (LWA): A Large HF/VHF Array
for Solar Physics, Ionospheric Science, and Solar Radar**

**A Ground-Based Instrument Paper for the 2010 NRC Decadal Survey of
Solar and Space Physics**

**Lee J Rickard, Joseph Craig, Gregory B. Taylor, Steven Tremblay, and
Christopher Watts**

University of New Mexico, Albuquerque, NM 87131

**Namir E. Kassim, Tracy Clarke, Clayton Coker, Kenneth Dymond, Joseph
Helmholtz, Brian C. Hicks, Paul Ray, and Kenneth P. Stewart**

Naval Research Laboratory, Washington, DC 20375

Jacob M. Hartman

NRC Research Associate, in residence at Naval Research Laboratory

Stephen M. White

AFRL, Kirtland AFB, Albuquerque, NM 87117

Paul Rodriguez

Consultant, Washington, DC 20375

Steve Ellingson and Chris Wolfe

Virginia Tech, Blacksburg, VA 24060

Robert Navarro and Joseph Lazio

NASA Jet Propulsion Laboratory, Pasadena, CA 91109

Charles Cormier and Van Romero

New Mexico Institute of Mining & Technology, Socorro, NM 87801

Fredrick Jenet

University of Texas, Brownsville, TX 78520

and the LWA Consortium

Executive Summary

The Long Wavelength Array (LWA), currently under construction in New Mexico, will be an imaging HF/VHF interferometer providing a new approach for studying the Sun-Earth environment from the surface of the sun through the Earth's ionosphere [1]. The LWA will be a powerful tool for solar physics and space weather investigations, through its ability to characterize a diverse range of low-frequency, solar-related emissions, thereby increasing our understanding of particle acceleration and shocks in the solar atmosphere along with their impact on the Sun-Earth environment. As a passive receiver the LWA will directly detect Coronal Mass Ejections (CMEs) in emission, and indirectly through the scattering of cosmic background sources. If coupled with a suitable transmitter, the LWA would be an excellent receiver for solar radar, potentially demonstrating accurate geomagnetic storm prediction from the Earth's surface. Both radar and passive receiving techniques could monitor the Sun-Earth environment during daytime as a complement to nighttime space weather remote sensing techniques.

The LWA will also naturally provide a measure of small-scale spatial and temporal ionospheric structure, a prerequisite for accurate calibration and imaging of solar and space weather phenomena. As a sensitive monitor of differences in total electron content (TEC) through the ionosphere, the LWA will provide an unprecedented characterization of ionospheric turbulence and waves, capable of testing predictions of global ionospheric models with an aim towards improving their accuracy through input to physics-based models. As a fully digital, multi-beaming instrument, the LWA can monitor the Sun daily with a dedicated solar beam, while simultaneously pursuing ionospheric and astrophysics science programs both day and night.

The planned LWA will consist of 53 phased-array "stations," each consisting of 256 pairs of crossed-dipole antennas, operating with Galactic noise-limited sensitivity over the frequency range 20–80 MHz. The stations will be distributed over the state of New Mexico, with maximum baselines (distances between stations) of up to 400 km, and nominally 16 stations in a 'core' within the central 10 km. Beam-forming (up to 4 simultaneous beams) will be done at the individual stations with the data then transmitted to a central correlator for image formation. The LWA will image wide fields of view with sufficient diversity of baselines to study both compact and complex sources in interferometric mode. The planned sensitivity in each beam will be a few mJy in 8 hours with a resolution of 8" to 2" (20 to 80 MHz). With a user-oriented operational concept and the goal to help stimulate University-based radio astronomy and hands-on student training, the LWA project embodies a 'science every step of the way' approach.

The first LWA station, LWA-1, will be complete at the start of 2011. LWA-1 will form four independent (in both frequency and pointing) beams on the sky, with instantaneous bandwidths of 8 MHz per beam, spectral resolutions down to 100 Hz, and temporal resolutions to 0.1 ms. Its homodyne receiver architecture will allow direct beam-formation over the entire LWA bandwidth. Operating as a fully electronic, phased array, the beams can be cycled rapidly among many sources on millisecond timescales. The science plan for the coming year includes several solar and ionospheric studies.

1. Introduction

The Long Wavelength Array (LWA, [2]) will be optimized for exploring the lowest electromagnetic window (~10 – 88 MHz) available for ground-based interferometric imaging, between the ionospheric cutoff and the FM bands. The LWA follows the heritage of the 74 MHz system developed by the Naval Research Laboratory and the National Radio Astronomy Observatory (NRAO) for the Very Large Array (VLA) radio-telescope [3]. That system was the first connected element, imaging interferometer to demonstrate sub-arcminute resolution imaging below 100 MHz. This breakthrough was achieved based on innovations in HF/VHF adaptive optics required to accurately measure and model small scale (temporal and spatial) ionospheric-induced phase variations that become severe on antenna separations (or interferometer baselines) > 5 km. The LWA is designed to extend the maximum baselines

available with the original 74 MHz VLA system (~35 km) by approximately one order of magnitude, and the available sensitivity by more than two orders of magnitude.

In the following sections we provide (§§ 2 and 3) a discussion of solar physics and heliospheric physics applications of the LWA, respectively; (§4) a review of LWA ionospheric remote sensing applications, afforded naturally through its requirement to calibrate against thousands of natural cosmic background sources; and (§5) a consideration of the LWA as a radar imaging receiver for detecting Earthward-bound Coronal Mass Ejections (CMEs) for geomagnetic storm prediction. In addition, we provide (§6) a brief technical overview of the LWA and its current construction status; and (§7) a summary of programmatic issues.

2. Solar Physics

The LWA frequency range, optimized for 20-80 MHz, is the domain of the classic solar radio burst types: Type II bursts, generated by shocks in the corona, with their characteristic fundamental-harmonic split-band structure; Type III bursts, drifting rapidly in frequency as the electron beams that generate them propagate into the solar wind; and Type IV bursts, from trapped electrons producing broadband emission in long-duration flares. Examples of Type II and IV emission are shown in Fig. 1; on a plot like this a Type III burst appears as a brief nearly vertical feature. With its sensitivity, flexible frequency coverage and multibeam capability, the LWA will be a powerful tool for the study of these bursts. Each of them is believed to emit by the mechanism of plasma radiation, *i.e.*, the conversion of electrostatic Langmuir waves into electromagnetic waves at the fundamental and second harmonic of the electron plasma frequency $9000 n_e^{0.5}$ Hz, where n_e is the electron density (cm^{-3}). The frequency of plasma emission thus reveals the density in the source. Some examples of possible solar science topics are described below.

An important advance provided by the LWA is the ability to image at many frequencies across a significant bandwidth simultaneously. Previous imaging of, *e.g.*, Type II bursts has been at fixed frequencies, and one then only has access to the phenomena that happen to be drifting through the observing frequency at any given instant. This is a disadvantage for Type II bursts because, as fig. 1 shows, they typically consist of fundamental and harmonic bands, each of which is split. It is believed that the splitting may be due to emission coming from the upstream and downstream regions of a shock, with the differing densities in the two locations leading to different plasma emission frequencies. Previously it has never been possible to make an image of the two split bands simultaneously: the LWA, with its large instantaneous bandwidth and the ability to image anywhere in that bandwidth, will make that possible and thus provide a test of models that use the splitting to infer the shock Mach number.

Similarly, fig. 1 shows that Type IV bursts exhibit strongly modulated emission. It is suggested that such emission comes from plasma emission that is broadband due to the range of densities experienced by

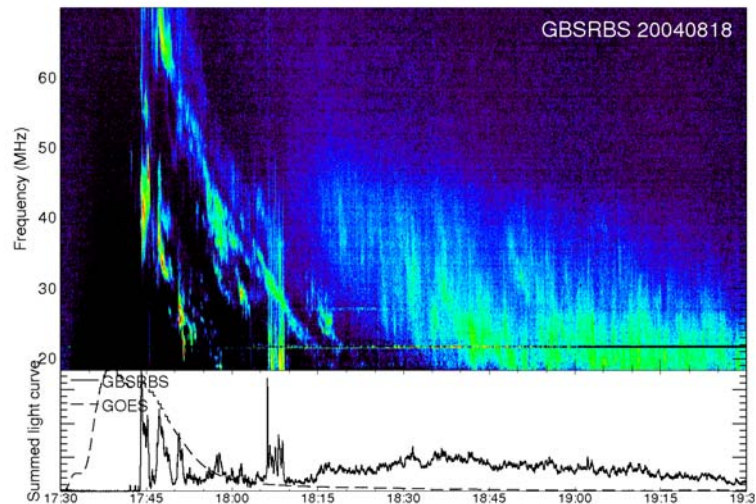


Figure 1: Radio emission from a solar flare in the LWA frequency range, observed with the Green Bank Solar Radio Burst Spectrometer. The upper panel shows a dynamic spectrum (frequency vs. time plot) with harmonic bands of a Type II burst dominating from 17:45-18:00 UT, and the broadband continuum of a Type IV burst drifting gradually lower in frequency from 18:20-19:30 UT.

electrons trapped in post-flare loops as they propagate along the length of the loops. The modulations then represent simultaneous injections of additional nonthermal electrons onto the loops. An alternative explanation is that the Type IV emission is composed of individual electron beams that drift rapidly over a finite height range. LWA-1, with its combination of exceptional sensitivity and time resolution, will be capable of looking for extreme drift rates in Type IV substructure across 8 or 16 MHz of bandwidth, while the full LWA system will be able to measure changes in source position with frequency and trace out the locus of the burst source.

In events in which the bright plasma emission sources are absent in some regions of the LWA's frequency coverage, it should be possible to detect CMEs directly via the synchrotron emission from electrons accelerated in the CME-driven shock above the solar corona. This has been demonstrated with Nançay Radioheliograph observations at 164 MHz by [4]. The emission by these electrons is generally weak relative to the bright coherent plasma emission of the classic large burst types, and does not show up on a dynamic spectrum such as fig. 1, but imaging reveals a quasicircular arc of emission co-located with the CME front. The spectrum of this emission close to the Sun [4] appears to be consistent with a nonthermal spectrum suppressed at low frequencies by the Razin effect. The LWA will be able to trace such emission to much greater heights above the Sun thanks to its lower frequency range; Razin suppression will be less effective at greater heights due to the lower densities in the atmosphere there, and the emission should be very bright and easily observed in the LWA frequency range provided that it is not swamped by plasma emission sources. These observations have the potential to address a large number of important questions in shock physics, including:

- What is the relative effectiveness of quasi-perpendicular and quasi-parallel shock acceleration?
- What is the magnetic field geometry of the expanding CME structure?
- How does the rate of electron acceleration vary with height and what is their energy distribution?
- What is the energy distribution of the accelerated electrons?

Related to this topic is the observation of “moving Type IV” bursts. These are huge, rare broadband disturbances in the LWA frequency range observed historically by the Culgoora Radioheliograph and (on a few occasions) by Clark Lake Radio Observatory; they cannot easily be distinguished from normal Type IV bursts from dynamic spectra alone, and there is debate as to whether their emission mechanism is plasma radiation or synchrotron. They are seen to move out to great heights above the solar surface at speeds similar to fast CMEs. However, their exact relationship to CMEs is poorly understood because there was only a brief overlap between modern space-borne coronagraph imaging of CMEs and the operation of Culgoora: in the one well-studied case, the moving Type IV burst appeared to be lagging behind the leading edge of the associated CME, lying closer to the densest material in the ejection (probably the erupting filament) [5]. The LWA will permit the observation of moving Type IV bursts again, and the study of their relationship to other erupting phenomena, for the first time in 25 years.

The LWA will also be capable of mapping the quiet solar atmosphere once sufficient stations in the core are available to provide good u - v coverage for a source of dimension 1° such as the Sun. Observing the variation in the structure of the solar atmosphere in the 1-3 R_{sun} height range will be an important adjunct to ongoing studies of the formation and acceleration of the solar wind, which is believed to occur in that height range. Currently a large emphasis is placed on MHD modeling and magnetic field extrapolation techniques to study these topics due to the difficulty of obtaining suitable measurements: The LWA's frequency flexibility will permit mapping of the solar atmosphere from 20 to 80 MHz and reveal changes in structure with height that will strongly constrain these studies.

3. Heliospheric Physics

The LWA will be able to employ the well-established technique of interplanetary scintillation (IPS) to track regions of increased density associated with CMEs as they propagate through the interplanetary medium. This technique is being used by several groups around the world (e.g., see <http://ips.ucsd.edu/>). The method is to observe the level of fluctuations (“scintillations”) in the signal from a bright background radio source as it passes through the solar wind: the fluctuations are produced by scattering and diffraction of the signal in the density fluctuations of the solar wind. The level of density fluctuations is generally found to be well correlated with the absolute density; a turbulent feature such as a CME-driven shock may well increase the level of scattering further.

IPS radio systems (e.g., STELab in Japan and Ooty in India, both at 327 MHz) generally employ large telescopes operated as single frequency ‘transit instruments’, where a set of strong compact radio sources is observed daily as the source transits the local meridian at the observing site. The advantage that the LWA possesses is that it has no moving parts: “pointing” is achieved electronically by phasing the signals from each of the 256 elements so that, when combined, they form a beam pointing at the source of interest. With up to 4 beams and its large collecting area, the LWA can observe 4 sources simultaneously with a time resolution of order milliseconds, opening up the possibility for unique data analyses. Since the LWA can switch to a new set of sources essentially instantaneously, it will be able to monitor the level of fluctuations in the solar wind with much denser time-and-space sampling than can be achieved with current instruments, with a consequent improvement in the ability to track the movement of discrete features in the solar wind such as CMEs. Furthermore, the LWA’s ability to make measurements over a significant frequency range simultaneously allows the use of frequency-correlation techniques that can yield velocity information even with a single station.

Initial work on IPS measurements can be carried out with LWA-1 using the classical IPS and frequency-correlation methods; once more stations are available, it will be possible both to add measurements of solar wind and density-structure velocities using the multi-station technique employed currently by STELab, and to use a denser array of scintillation sources thanks to the smaller beam of the multi-station array.

The ability to measure polarization adds an extra dimension to both IPS and other observations. The polarization of the CME synchrotron emission observed by [4] will be of great interest for revealing the structure of the magnetic field in an expanding CME front. Further into the heliosphere, Faraday rotation measurements can be used to infer magnetic fields: such measurements require measuring changes in the full polarization state of background radio sources as a CME passes in front of them, and the variation of the polarization with frequency. These are difficult measurements and this is not a prime goal of the LWA, but this technique will be explored once the LWA has sufficient sensitivity and has measured the polarization characteristics of its stations.

4. Ionospheric Physics

The distribution of electric charge in the Earth’s ionosphere perturbs the refractive index for radio waves passing through it, and these refractive index fluctuations change the phase velocity of the rays and thus introduce delays between different paths. This effect makes a multi-element low frequency array extremely sensitive to small *differences* in total electron content (ΔTEC) through the ionosphere, as defined by the separation of interferometer pairs sampling it [1,2]. Typical ionospheric remote sensing techniques sample ΔTEC at the 0.1 TECU level (1 TECU = 10^{12} electrons* cm^{-2}) and on spatial scales of ≥ 100 km. The VLA can measure ΔTEC at the milli-TECU level and on spatial scales approaching 100 m. The VLA has been used for 330 MHz-based studies of travelling ionospheric disturbances (TIDs) [6], while more recent studies have extended measurements to lower frequencies [7].

The LWA will be a far more powerful ionospheric probe than the VLA, coupling the technical advantages of much greater collecting area, spatial sampling, and broadband low frequency spectral

coverage with electronic multi-beaming and continuous monitoring. While on the one hand the ionosphere will be a significant problem for the LWA astrophysical observations, this “problem” offers a tremendous opportunity for ionospheric science studies and serves as a major justification for the instrument. The electron content of the ionosphere above the LWA, varying with position, height and time, introduces phase delays in the signal paths from the sky to the telescope. These delays show up to lowest order as a simple position shift of a source on the sky, and to

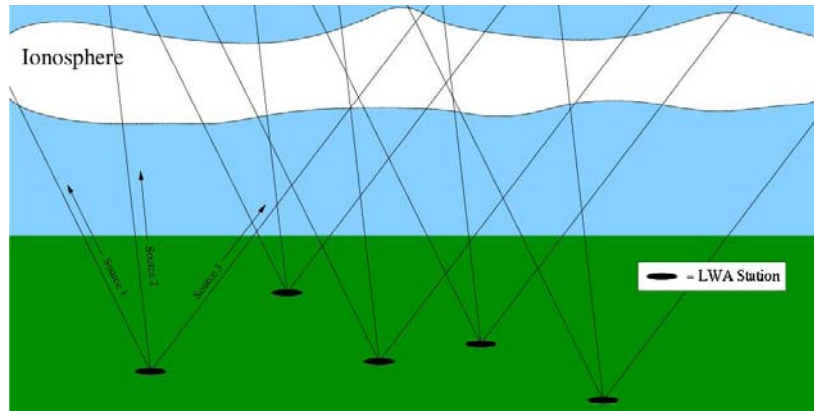


Figure 2: A schematic illustration of LWA ionospheric tomography. With electronic steering, multiple beams and high sensitivity, the LWA can image 100 cosmic background sources within 5 seconds. Here, 5 stations and 3 sources yield 15 lines of sight. 53 LWA stations will provide 5,300 pierce point samplings through the ionosphere.

second order as a smearing of the source, but over the long baselines planned eventually for the LWA this is an inadequate description of ionospheric effects: they will be different in different parts of the sky, and for the same source viewed from different stations. The LWA can therefore provide unparalleled measurements of TEC fluctuations simultaneously from small (~1 km; ~milli-TECU) to large (~400 km; ~TECU) scales, a combination of synoptic and detailed views that no other instrument can approach. Furthermore, it will do it as a matter of course, as a pre-requisite for accurate calibration and imaging of the Sun and other cosmic radio sources. And, as a real-time ionospheric monitor, the LWA support tests of the predictions of global ionospheric models, with an aim towards improving their accuracy through input to physics-based models.

From a single LWA station, the ionosphere can be studied by rapidly cycling through a set of strong compact sources that cover the sky down to some elevation and measuring the delay for each line of sight by established methods (fig. 2). As for the IPS application, the fact that the LWA has multiple beams and no moving parts, so that repointing the beams can be achieved almost instantaneously, allows such studies to be carried out with unprecedented time sampling. Ionospheric perturbations such as “sudden ionospheric disturbances” can be detected as position-varying phase shifts depending on the electron content along each line of sight. Mapping these changes in electron content with time allows one to see the movement of features overhead.

With multiple LWA stations, measuring the electron content towards the same source in the sky from different stations introduces 3-dimensional information: the height distribution of the electron content can be studied from the differences of different lines of sight (fig. 2). The baseline range of the full LWA, 400 km, is ideal for sampling the full height range of the ionosphere by this tomographic technique, potentially providing thousands of measurements through the ionosphere on timescales of seconds or less. The combination of measuring small and large spatial scales simultaneously, coupled with three-dimensional information and high time resolution, means that the LWA has the potential to improve greatly our understanding of the dynamics of the fine-scale structure of the ionosphere.

Ionospheric studies with just a single LWA station can contribute indirectly to magnetospheric physics. Recent experimental evidence shows that wave-particle interactions are significant factors in both beta acceleration and beta loss in the natural radiation belts [8]. Among the natural processes that are now known to induce electron precipitation are lightning, through generation of whistler-mode waves [9], earthquakes, by generation of ultra-low-frequency (ULF) and very-low-frequency (VLF) waves [10], and the direct distortion of the magnetosphere by solar flares and coronal mass ejections (CMEs) [11].

The precipitating electrons cause localized ionization and changes of ionospheric plasma conductivity [12]. This results in enhanced absorption of the cosmic high-frequency (typically 10 – 60

MHz) radio background, originating primarily in the D-region. Such enhanced, or anomalous, absorption measurements have been the subject of ground-based studies since before the original International Geophysical Year [13]. The method currently used for such studies is riometry, and has remained relatively unchanged for almost as long [14]. A long time-series of observations is used to determine a ‘quiet background level’, which is a convolution of the system response and the (strong) Galactic background, and varies slowly on an hourly and yearly basis. Anomalous absorption measurements are detected as shorter term variations in which the observed flux drops, perhaps by tens of dB.

The standard riometric measurement is made at a single, relatively narrow bandwidth. With the LWA, however, we can provide measurements over a broad range of frequencies, in the 10 – 80 MHz range. Furthermore, the system can be calibrated so that, rather than having to derive a ‘quiet background level’ from the data, the absolute sky brightness against which the absorption is measured can be determined. These are both significant enhancements of the methods for studying anomalous absorptions. Additional information can be gleaned from the spatial distribution of the absorption event. To date, this has been done by using small arrays of antennas (typically 4x4 or 8x8) and analog beam formation (via Butler matrices), to generate a set of beams on the sky at fairly coarse spatial resolution.

5. Solar Radar

The LWA could potentially provide an important new capability as a receiving array for radar studies of the solar corona. The solar radar concept was first proposed as an approach to investigating the ionized structure of the solar corona [15, 16]. Among the early experiments, echoes were reported both from Arecibo [17] and El Campo [18]. The El Campo campaign extended from 1961-1969, and its published reports are the main comprehensive description existing of solar radar echoes.

The El Campo solar radar operated at 38 MHz with a total power of 500 kW and used an array of antennas of about 18,000 m² in size, both to transmit and to receive. The fan-shaped beam of the El Campo radar was about 1° x 6° in the NS x EW direction, allowing only one transit experiment of the sun per day to be conducted. An experiment consisted of a coded waveform transmitted toward the sun for 16 minutes (the round-trip travel time of light) followed by 16 minutes of reception. The data recorded during the reception time interval were then correlated with the transmitted code to search for signals at time delays and frequency shifts expected for a solar echo at the reflection level of 38 MHz, expected at about 1.4 R_o (where R_o is the solar radius). From those cases in which an echo could be identified at some level of statistical probability, a radar cross section of the sun was calculated. The majority of radar cross sections had values about equal to or slightly larger than the solar geometric cross section. However, over the years of the El Campo experiments, there emerged a subset of cross sections that appeared at earlier time delays. It was suggested that these “high corona echoes” might be related to dense irregularities possibly associated with shock fronts in the corona [19].

Today we recognize that these high corona echoes could have been produced by large scale coronal disturbances such as Coronal Mass Ejections, a phenomenon that was unknown to solar physicists of the 1960s, but which today is recognized as a major driver of space weather at the earth. Thus, interest in the use of solar radars was revived in the 1990s [20] when it was recognized as a possible technique for early detection of earthward-moving CMEs.

Fig. 3 illustrates the concept of using a solar radar to detect an earthward-moving CME while it is still near the sun. The leading front of the CME is expected to cause a frequency shift in the radar echo proportional to the velocity of the CME, from which the travel time to the earth can be derived. However, today there is no extant solar radar comparable to El Campo, which was de-commissioned long ago (perhaps a memorial to being ahead of its time). Several high power transmitter facilities are in use today that approximate some characteristics of a solar radar. However, because these facilities were designed and built for a different purpose, they all lack some crucial aspect needed for a true solar radar.

Among the existing facilities are Over-The-Horizon (OTH) radars, which have power levels and frequencies comparable to those of the El Campo radar, but have antenna beams that are hard-pointed at

low elevation angles and azimuths and unable to illuminate the sun except on a few days of the year. Another class is the high power ionospheric heating transmitters, which have powers in some cases exceeding the power of the El Campo radar, but operate only at the low frequencies designed to maximize interaction with the earth's ionosphere. Only at special times when the ionospheric cutoff frequency is low enough are these transmitters able to illuminate the sun. Other high power ionospheric radars have fixed pointing directions or operate at frequencies too high for solar

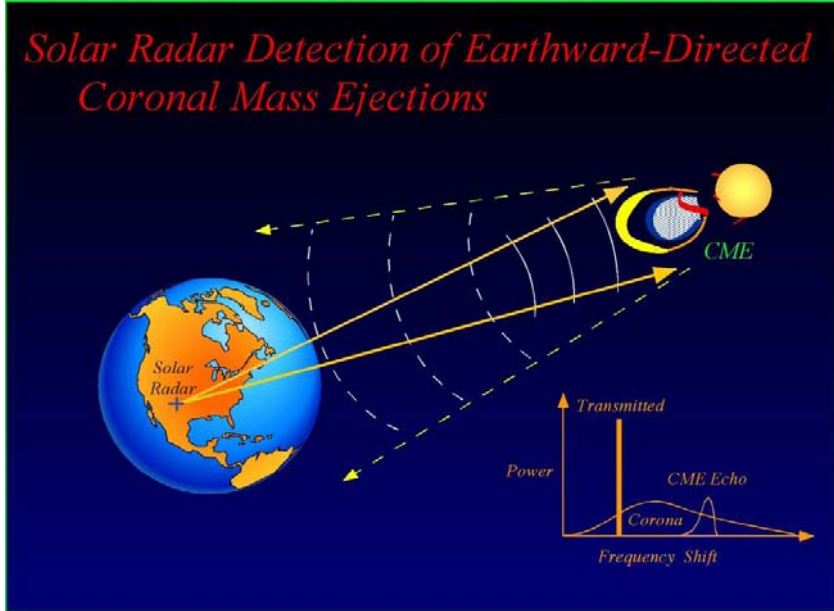


Figure 3: The concept of using solar radar to measure CME velocity and travel time to Earth.

radar. Although these facilities were not designed to be solar radars, several experiments have been done with them anyway, in configurations that are as close as possible to the El Campo radar. Among these experiments, frequencies of 9 MHz, 25 MHz, 40 MHz, and 50 MHz have been used. However, the results have been somewhat disappointing, with no evidence of a well-defined echo. The most recent solar radar experiments have been unable to clearly detect solar echoes [21].

Thus it remains an important task to understand the limitations that may have been significant in these various attempts to reproduce the El Campo solar radar experiments. It is possible that solar radar experiments, already intrinsically difficult, are not adequately addressed with existing facilities and that a true solar radar is required.

While a solar radar demands high power transmission (radiated power up to 3 MW is desirable) due to the great distance to the sun and to the natural radio noise environment of the sun, it is just as important that the receiving array be well-matched to the angular size of the target and be able to resolve spatial and temporal variations in the echo and background emissions.

The LWA will receive frequencies in the range of 20 to 80 MHz and can provide several beams to receive several frequencies simultaneously, providing a significant improvement to the receiving component of a solar radar; all previous solar radars involved only one frequency. The LWA is being designed with solar studies in mind and will use modern techniques of digital signal processing of the data. The array will have electronic phasing of antennas in the various sub-arrays (or stations) situated over a large area. The spatial extent and phasing of the LWA bring about two important characteristics needed for a solar radar: beam sizes comparable to and smaller than the angular size of the solar disk (~ 30 arc-min) and the agility to form and track one or more beams to follow the sun across the sky. Neither of these capabilities existed in previous solar radars, including those of El Campo. All previous solar radar experiments have been done in transit mode in which the sun drifted across a stationary beam. The small beam size of the LWA will allow it to receive its signals from a solid angle that includes only the sun or to utilize smaller beam widths to map structure in the echo signal across the solar disk. The tracking capability expands the solar radar experiment to several hours, allowing more experiment cycles on a given day. The basic cycle is about one-half hour, composed of 16 minutes of transmission followed by 16 minutes of reception. As mentioned above, El Campo conducted only one experiment cycle per day. The experiment cycle time corresponds to an angular displacement of the sun by about 8°, requiring a stationary beam width to be broad enough to maintain sufficient antenna gain on the sun. The beam of

the LWA phased array can be electronically steered to track the sun for several hours per day, thus making possible several experiment cycles per day. In addition, the LWA beam maximum response can be kept centered on the sun throughout the time of tracking. The additional cycles possible with the LWA can be used to help discriminate against solar radio noise that may resemble a radar echo.

6. Technical Overview

The LWA will take advantage of emerging technologies in calibration, imaging and digital processing to surpass previous instruments by several orders of magnitude in resolution and sensitivity below 100 MHz. The LWA will consist of 53 phased-array “stations,” each consisting of 256 pairs of crossed-dipole antennas, operating with Galactic noise-limited sensitivity over the frequency range 20–80 MHz. The stations will be distributed over the state of New Mexico, with maximum baselines (distances between stations) of up to 400 km, and nominally 16 stations in a ‘core’ within the central 10 km (Fig 4). Beam-forming (with up to 4 independent – both in frequency and pointing – simultaneous beams) will be done at the individual stations, with the data then transmitted to a central correlator for image formation. Its homodyne receiver architecture will allow direct beam-formation over the entire LWA bandwidth, with instantaneous bandwidths of 8 MHz per beam, spectral resolutions down to 100 Hz, and temporal resolutions to 0.1 ms. The LWA will image wide fields of view with sufficient diversity of baselines to study both compact and complex sources in interferometric mode. The planned sensitivity in each beam will be a few mJy in 8 hours with a resolution of 8" to 2" (20 to 80 MHz).

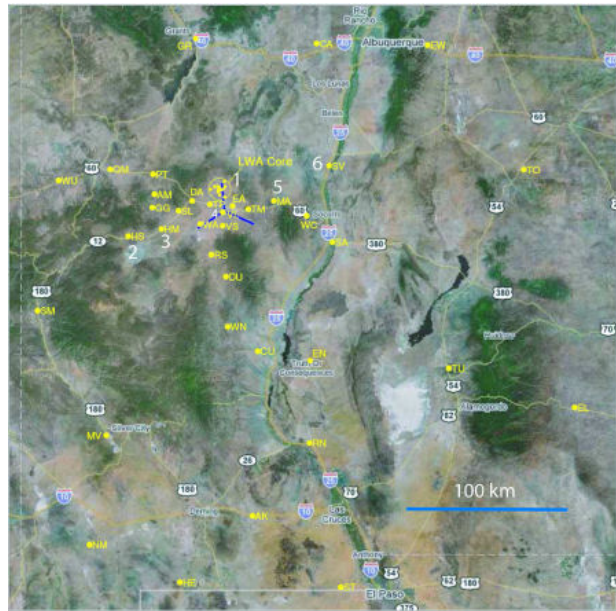


Figure 4: Nominal LWA station locations shown in yellow; location of the VLA is shown in blue.

The first station (LWA-1) will be complete at the start of 2011. Tests with the analog system already show that there are no unanticipated problems in meeting performance expectations. It is anticipated that the design of the additional stations will be similar to that for LWA-1, as described below.



Figure 5: Aerial view of LWA-1, showing stand layout and (lower right) electronics shelter.

Receiving Elements and Station Layout:

The primary receiving element is a fixed stand that incorporates two broadband, crossed, linearly-polarized dipoles. A group of 256 stands will form a roughly 100-meter diameter station, with a pseudorandom distribution (fig. 5) to prevent aliasing of the main lobe and to mitigate large sidelobes at higher frequencies where the aperture will be undersampled. The station beam can be steered to any point in the sky by adjusting the digital delays of the individual elements. Beam steering will be entirely electronic.

Each dipole (Fig. 6) feeds a balanced-input active-balun to produce a single-polarization, Galactic-noise-dominated output signal. The front end electronics (FEE; Fig. 7) uses commercial InGaP HBT MMIC amplifiers (Mini-Circuits GALI-74) in a differential configuration presenting a $100\ \Omega$ balanced load to the antenna. This is followed by a 180° hybrid, a fifth order RFI rejection filter, and an additional 12 dB gain stage (Mini-Circuits Gali-6) to produce a $50\ \Omega$ single-ended signal suitable for transmission over coaxial cable. The gain, noise temperature, and input 1-dB compression point are approximately 36 dB, 250 K, and -18 dBm respectively, roughly independent of frequency over 10–88 MHz. The FEE circuit board has been designed to enable identical signal polarization units to be assembled back-to-back, forming a dual polarization FEE. A coarse-mesh ground screen underneath the stand will reduce ground losses and stabilize the antenna impedance.

The choice of 256 stands distributed over ~ 100 m is driven by the anticipated need to rapidly image several hundred sources across the sky, to calibrate for ionospheric effects within the station field of view (FWHM $\sim 8^\circ$ [20 MHz/v]). It meets the sensitivity goals of the science requirements while achieving a balance with classical and sidelobe confusion for 400-km baselines over plausible integration times. It also balances cost against quality of image calibration over a broad range of frequencies and zenith angles.

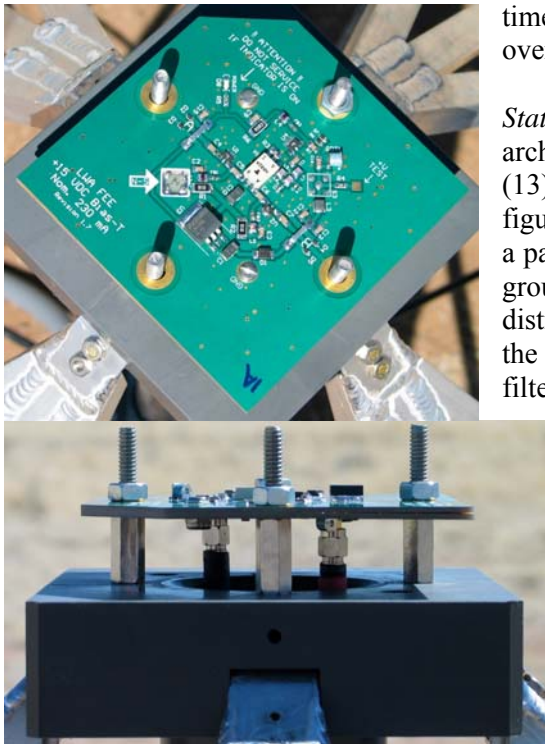


Figure 7: (Top) FEE viewed from above; (Bottom) FEE pair viewed from side.



Figure 6: Antenna stand in field.

Station Architecture and Electronics: Figures 8-9 summarize the architecture of the station; (10-12) are the basic signal path, and (13) is the common monitor and control system (MCS). In figure 5, signals from the 256 stands (STDs), each consisting of a pair of antennas (ANT) and front-end electronics (FEE) over a ground screen (GND), go by way of a common RF and power distribution network (RPD) to the signal-entry panel (SEP) of the electronics shelter (SHL). Inside, each polarization is filtered and amplified by an analog receiver (ARX) and then

direct-sampled at 196 Msps by the A/D converter in figure 9. We are adopting a digitization scheme that enables us to fold the FM band (88-108 MHz) over on itself, substantially reducing its impact. This fixes a high-frequency limit of 88 MHz and a low-frequency limit of 10 MHz.

In figure 9, the beam-forming units (BFUs) employ a time-domain delay-and-sum architecture, which allows the entire 10-88 MHz passband from each antenna to be processed as a single wideband data stream. Delays are implemented in two stages: A coarse delay is implemented using a first-in first-out (FIFO) buffer operating on the A/D output samples, followed by a finite

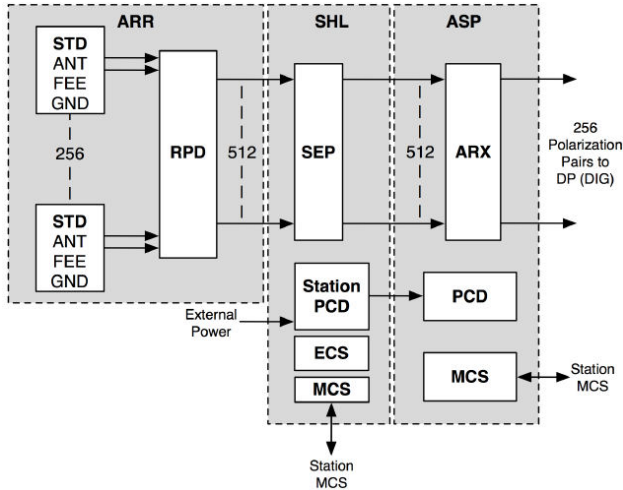


Figure 8: Architectural schematic of LWA from the antennas through the analog signal processing.

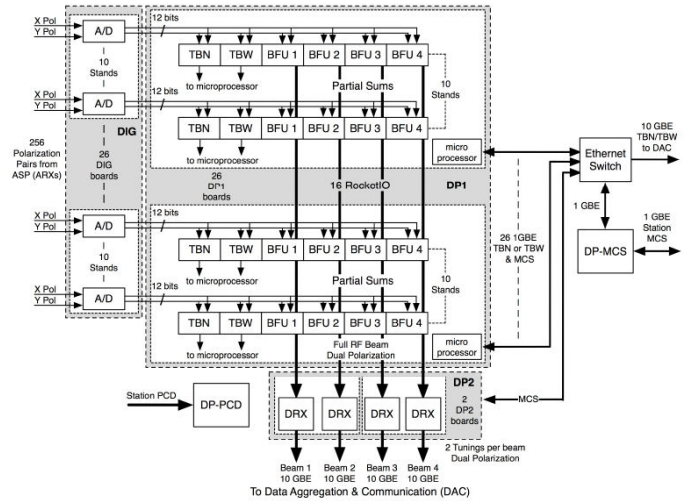


Figure 9: Architectural schematic of LWA electronics, from digitization through digital processing.

impulse response (FIR) filter for sub-sample delay. The signals are then added to the signals from other antennas processed similarly. Four dual-polarization beams of bandwidth 78 MHz, each capable of fully independent pointing over the visible sky, will be constructed in this fashion. Each full-bandwidth beam is down-converted by a digital receiver (DRX) and sent to a polyphase filter bank to channelize the beams into spectral channels. With 4096 channels, beam bandwidths up to 8 MHz and spectral resolution down to 61 Hz are achieved.

These beams will be available for various “backends” implemented at the station level, such as data recorders, wideband spectrometers, and pulsar machines. For interferometric imaging, two “tunings” will be extracted from any frequency in the 78 MHz-wide passband for each beam. These beams are the output to the LWA correlator. In addition, stations in the LWA core will output a wideband beam derived from one of the full-RF beams.

To facilitate commissioning activities, diagnostics, and certain types of science observations requiring all-sky fields of view, the station electronics will also have the capability to coherently capture and record the output of all A/Ds, where each A/D corresponds to one antenna. This will occur in two modes: the “transient buffer – wideband” (TBW) allows the raw output of the A/Ds to be collected continuously for 57 ms at a time. The “transient buffer – narrowband” (TBN) allows a single tuning of 1 kHz to 100 kHz bandwidth to be streamed continuously.



Figure 10: Analog signal processing board

For the first LWA station, the data streams will be handled by a set of data recorders (MCS-DR), as shown in figure 12. The MCS-DR consists of 5 identical computers, four of which receive data streams from the digital processor (DP) corresponding to the output of each of the four station beams. The fifth computer receives the DP output data streams corresponding to TBW/TBN outputs. All computers contain internal arrays of large hard drives, to which data can be streamed at the rate received from the DP.

Data Handling and Correlator:



Figure 11: Digital processing board

The data aggregation and communication system (DAC) for the full LWA will be a Gigabit ethernet over optical fiber connecting stations to the correlator at a central location. For most stations, the output to the correlator will be both polarizations of 3 beams of 8-MHz bandwidth each, resampled to 8 bits at 1.5 times the Nyquist rate. This results in a data rate of 576 Mb/s. One of these beams will always be available to assist in measuring the ionosphere, as part of image calibration, whereas the other two can be used for simultaneous independent observing programs. Practical limitations in data transmission from the stations to the correlator constrain the immediate plan for multibeam operation to a bandwidth of 8 MHz (selectable within the tuning range). However beams will be formed at the station as “full RF”;

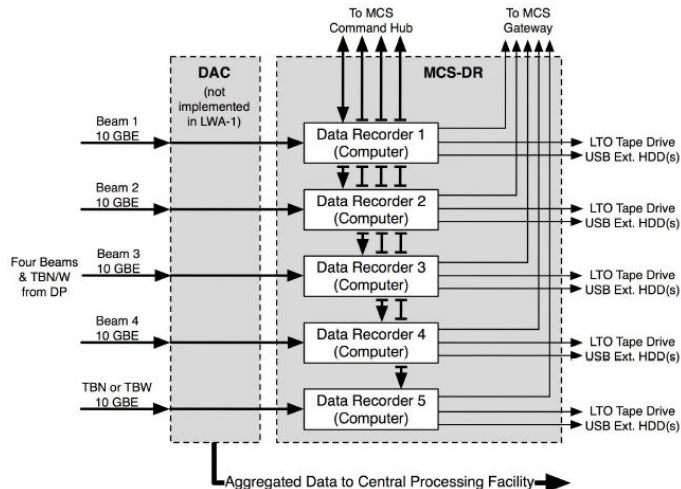


Figure 12: Architecture of LWA data recording.

i.e., with bandwidth equal to the tuning range. LWA core stations will also transmit a wideband beam (~56 MHz) to the correlator simultaneously with the three 8 MHz beams. This beam will be used primarily for solar science during the day and for early universe (“Dark Ages”) studies at night.

The large number of high data-rate signals involved makes correlation extremely computationally-intensive, requiring dedicated equipment running in real time for the complete LWA. This is not the case for LWA-1. The early LWA is rather in the regime of VLBI – a small number of stations and a moderate bandwidth to be correlated. Thus, we need merely capture the station outputs at a central location using disk buffers, and perform correlation in software using general-

purpose computers, using a system like DiFX [22]. We intend to build a small computer cluster, using 3 AMTF MTG15400Duo servers to host a software correlator for the few-station LWA. These units can easily handle the standard station data rates of 576 Mb/s, and can even cope with the full bandwidth output of a single station: 1 Gb/s for each of four beams, plus 1 Gb/s for the narrowband transient buffer.

Control Systems: The station MCS (Fig. 13) is essentially the set of computers that controls the station, and provides status information. Various subsystems including the analog and digital processors also have MCSs, which are embedded computers subordinate to the station MCS. The subsystem MCSs are implemented to facilitate modularity in the station design and to facilitate independent development of subsystems. The Scheduler is a computer whose primary function is to issue commands and receive status from other LWA subsystems. It handles tasks that are extremely time sensitive and that must be coordinated on timescales down to milliseconds. The Executive is the computer which exercises top-level control over MCS as well as the station. It is responsible for interpreting observation requests and, from these, generating the data which becomes the content of command messages issued by the Scheduler. This includes numerically intensive operations such as computation of FIR-filter coefficients. The Executive manages tasks that are moderately time-sensitive and that must be coordinated on timescales down to

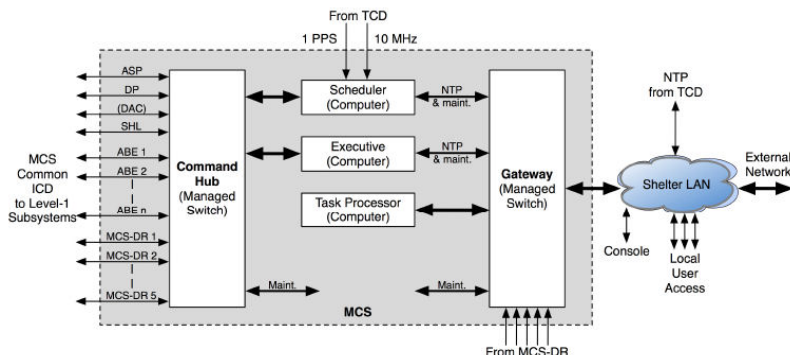


Figure 13: Architecture of LWA monitor and control system.

seconds. The Task Processor is a computer which exists primarily to host applications that are not time critical (time resolutions > 1 sec), and therefore can be offloaded to reduce the processing burden of the Executive. It is the primary interface with users, managing command line and GUI interactions. The Task Processor is also responsible for the scheduling and interpretation of internal diagnostics (either automatic or user-directed), and manages MCS-DR.

Radio Frequency Interference: A sense of the RFI environment is conveyed by figure 14, which shows the observed sky signal obtained in the field with the actual antenna, front-end electronics, and analog receiver. The result is sky-noise dominated by at least 6 dB over the range 20–80 MHz, and by at least 10 dB over 28–47 MHz. The impact of very strong RFI at the lowest part of the band has been minimized through use of a split-gain configuration of the ARX. Note that the major RFI features usually seen above 40 MHz, from analog TV signals, have now essentially vanished at the site, thanks to their move to digital TV carriers at higher frequencies.

Experience from the 74-MHz VLA system and other instruments has demonstrated that RFI from external as well as internal sources will be present at all levels throughout the spectrum. Having demonstrated that the strongest local RFI does not threaten linearity, we can be confident that the primary difficulty will be the increase in the amount of manual effort required to reduce data. A variety of solutions for automatic real-time mitigation of RFI are being considered for implementation. In the station electronics, this may include the ability to modify the responses of digital filters to suppress narrowband RFI, and pulse blanking to remove strong, bursty interference. Spatial or space-frequency nulling can be supported by the electronics architecture. For spectrometry, time-frequency blanking to resolutions of a few ms \times a few kHz is supported. Other devices and backends may use additional application-specific methods, and the specific mix of techniques employed will depend on the observing mode and RFI present.

Ionospheric Calibration: The early LWA stations will have baselines of tens of km. These are comparable to baselines that have been used at the VLA at 74 MHz, so that we have reasonable expectation of being affected by the same phenomena as seen at the VLA. Ionospheric calibration will be done with a ‘flickering’ method (cf. §5 below), which consists of rapidly cycling through and imaging the several hundred celestial radio emitters (sources) that we predict will be isolated enough to be imaged with standard calibration techniques. Such sources can therefore function as ionospheric calibrators, because calibrating to them determines the differences in ionospheric column density (Total Electron Content differences, or Δ TEC) along the lines of sight from each LWA station towards each calibrator source. An analysis based on VLA Low-frequency Sky Survey (VLSS, [23]) fluxes and LWA antenna simulations shows that, at 74 MHz, roughly 100 calibrator sources can be observed at any single time, which is far greater than the number of instantaneously available GPS or similar satellite beacons. This process can be done within a cycle time of 6 to 7 seconds, with an average of 50 msec per source. In addition to providing calibration, it provides the essential data to generate a dynamic, all-sky model of the ionosphere rich in phenomenology.

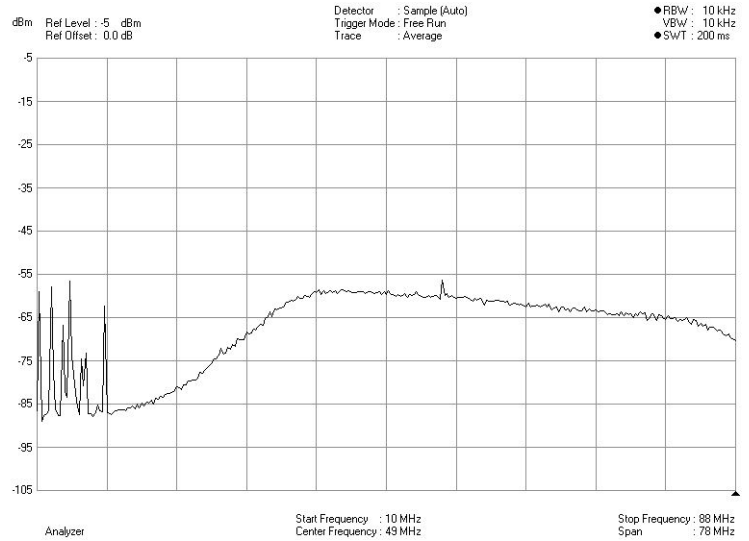


Figure 14: Spectrum acquired in the field using the LWA active antenna, FEE, and ARX, as described in the text. The gain for the lower part of the band has been reduced to minimize the impact of RFI at the lowest frequencies.

The key issue preventing tests of this method with LWA-1 is the confusion noise limit for a single station, which is reached in ~ 1 msec. By providing ‘outrigger’ baselines, to antennas significantly outside LWA-1, this confusion noise can be reduced significantly.

An indication of the scale of ionospheric fluctuations has been derived from VLA 74 MHz observations of Virgo A [24]. The amplitudes and spatial extents of the apparently turbulent structures seen during the night are similar to those of tropospheric phase fluctuations seen in the visible by optical interferometers [25]. That, together with the scanty sampling of station spacings, puts the full LWA imaging more in the regime of the optical interferometer than more densely sampled systems like the VLA. In this regime, phase closure ‘imaging’ (really more like model-fitting) is possible on bright sources [26,27], suggesting that the early phases of the LWA can operate in this mode.

The ultimate operational characteristics of the LWA are summarized in Table 1.

Table 1: LWA Operational Characteristics

Frequency Range	10-88 MHz (20-80 MHz optimized)
Effective Collecting Area	10-30 MHz: $\sim 10^5$ m ² ; 30-88 MHz: $\sim 10^5 (30 \text{ MHz}/\nu)^2$ m ²
Dipole Elements Total / Dipoles Per Station	$\sim 10^4$ / 256
Number of Stations / Station Diameter	~ 53 / ~ 100 m
Station Interferometer Baseline Range	0.1-400 km
Point Source Sensitivity (dual polarization, 1 hour integration, 4 MHz BW)	1.0 mJy @20 MHz, 0.5 mJy @80 MHz
Angular Resolution	15'' @ 10 MHz; 5'' @ 30 MHz; 2'' @ 80 MHz
Field of View	$\sim 2^\circ$ @ 80 MHz (proportional to ν)
Number of Independent FOV (beams)	4
Maximum Observable Bandwidth	~ 20 MHz/beam
Spectral Resolution	≤ 1 KHz
Image Dynamic Range	$\geq 10^4$
Digitized Bandwidth	Full RF

7. Programmatic Issues

The LWA Project is funded through a contract from the Office of Naval Research to the University of New Mexico, which partners directly with the Naval Research Laboratory, Virginia Tech, the Jet Propulsion Laboratory, Los Alamos National Laboratory, and the University of Iowa. In addition, the National Radio Astronomy Observatory, the Air Force Research Laboratory, and New Mexico Tech participate on the LWA Executive Committee.

The Project is now moving into two concurrent phases. The first is commissioning, validation, and scientific operation of LWA-1. This phase will include validation of performance; determination of methods for calibration, correlation, and imaging; and application to a suite of scientific problems, including studies of solar bursts, Jupiter bursts, and ionospheric turbulence and absorption events. The second phase is construction of new stations based on the LWA-1 design, incorporating design changes driven by LWA-1 commissioning results, and operation of the growing array. After validating the station systems in LWA-1, we will construct stations according to the optimal configuration [28, 29]. After completing the first three stations, we will test closure phase methods. There is a planned pause at completion of the first ~ 13 stations, with which we will be able to execute a full-scale proof of principle of complex imaging through the ionosphere and with simultaneous extraction of useful ionospheric data. There is, however, no intrinsic reason why, with subsequent funding, we cannot grow the array to the final 53-station instrument while operating it as an active scientific instrument. Nor is there any

insuperable barrier to using more funds during the first four years to build more than the 13 stations in this plan. A detailed analysis of this case was made for the Astro2010 Decadal Review [30].

The cost of completion depends on the pace at which additional stations are built. Given the advanced state of construction of LWA-1, we have a fairly confident estimated cost of parts and ground preparation of ~\$750K/station, and 5,000 hours (2.5 FTE) of construction labor. At a pace of 4 stations/year, and including the cost of making connections to power and data fiber, we arrive at a rough estimate of \$1M/station for costs outside construction labor, and ~\$1.2M/station with labor.

The operating cost is driven by power and communications; our estimate is \$51K/station/year. The maintenance cost is \$38K/station/year, based on very rough reliability figures for the station components. However, at least one major real-world issue – failure rates due to lightning – has not yet been factored in. This component obviously grows with the number of operating stations.

The location of the LWA in New Mexico enhances synergies with two major players in RF studies of space physics. Because the LWA will provide a unique data source for information on the structure and dynamics of the ionosphere at scales from hundreds of kilometers down to hundreds of meters, on timescales of minutes, and with a precision exceeding that of other current measurement techniques, AFRL recognizes that it can be an important asset to studies of ionospheric scintillation and refraction, affecting a wide variety of space-based systems. The LWA is also seen as an important asset for solar studies. The AFRL Space Weather group is currently providing support for students and postdoctoral fellows, establishing joint research projects between its personnel and UNM faculty, and represented on the LWA Executive Committee.

In addition, the NSF/AUI National Radio Astronomy Observatory is also represented on the LWA Executive Committee. NRAO hosts the first LWA station at the Very Large Array and works with UNM on low frequency radio astronomical techniques. NRAO has been an important source of advice, both in the technical arena (receiver development, site development, radio-frequency interference, data communications) and in the science.

Finally, we note the potential utility of LWA data for the requirements of defense, national, civil, and commercial space systems. Navigation (GPS, WAAS) and communications systems suffer deterioration and even outages because of small-scale ionospheric structures; thus, the ability to predict their occurrence and extent is needed. DoD global assimilating ionospheric models (comparable to modern numerical weather prediction models) require estimates of sub-grid structure that few instruments other than the LWA could provide. Space-based attempts to geolocate tactical radio emitters (many in the HF band) require corrections for refractive offsets due to these small-scale structures. Space-based radars operating in the VHF (for foliage penetration) and in the HF (for ground penetration) require similar refractive corrections, and must also be able to make coherent two-dimensional images. Over-the-horizon radars for very precise long-range target detection and tracking, as well as for large-scale ocean surface current measurements, need to calibrate the ionospheric mirror at fine levels. Operationally responsive space assets that require good ionospheric propagation conditions (for tactical geolocation, communications, and other aspects discussed above) will need to predict ionospheric ‘weather’ sufficiently well to support mission planning; this requires an understanding of how ionospheric dynamics leads to small-scale structure, as will be studied by LWA.

8. References

1. Kassim *et al.* 2010, ‘The Long Wavelength Array (LWA): A Large HF/VHF Array for Solar Physics, Ionospheric Science, and Solar Radar’, *Proceedings of the Advanced Maui Optical and Space Surveillance Technologies Conference*, Sept 14-17, 2010, Maui, Hawaii.
(<http://www.amostech.com/TechnicalPapers/2010/Posters/Kassim.pdf>)
2. Ellingson *et al.*, ‘The Long Wavelength Array,’ *Proceedings of the IEEE*, **97**, 1421-1430, 2009.
3. Kassim *et al.*, ‘The 74 MHz System on the Very Large Array,’ *The Astrophysical Journal Supplement Series*, **172**, 686-719, 2007.
4. Bastian *et al.*, ‘The Coronal Mass Ejection of 1998 April 20: Direct Imaging at Radio Wavelengths,’

- The Astrophysical Journal*, **558**, L65-L69, 2001.
5. Stewart *et al.*, 'Visible light observations of a dense plasmoid associated with a moving Type IV solar radio burst,' *Astronomy and Astrophysics*, **116**, 217-223, 1982.
 6. Jacobson and Erickson, 'Observations of electron density irregularities in the plasmasphere using the VLA radio interferometer,' *Annales Geophysique*, **11**, 869-888, 1993.
 7. Cohen and Röttgering, 'Probing Fine-Scale Ionospheric Structure with the Very Large Array Radio Telescope,' *Astronomical Journal*, **138**, 439-447, 2009.
 8. Vainio *et al.*, 'Dynamics of the Earth's Particle Radiation Environment,' *Space Science Reviews*, **147**, 187-231, 2009.
 9. Bucik *et al.*, 'Satellite observations of lightning-induced hard X-ray flux enhancements in the conjugate region,' *Annales Geophysique*, **24**, 1969-1976, 2006.
 10. Pulinet, *et al.*, 'Main phenomenological features of ionospheric precursors of strong earthquakes,' *Journal of Atmospheric and Solar-Terrestrial Physics*, **65**, 1337-1347, 2003.
 11. Orsolini *et al.*, 'An upper stratospheric layer of enhanced HNO₃ following exceptional solar storms,' *Geophysical Research Letters*, **32**, L12S01, doi:10.1029/2004GL021588, 2005.
 12. Demirkol *et al.*, 'Ionospheric effects of relativistic electron enhancement events,' *Geophysical Research Letters*, **26**, 3557, 1999.
 13. Mitra and Shain 1953, *J. Atm. Terr. Physics*, **4**, 204.
 14. Little and Leinbach 1959, *Proc. IRE*, **47**, 315
 15. Kerr, 'On the possibility of obtaining radar echoes from the sun and planets,' *Proceedings of the IRE*, **40**, 660, 1952.
 16. Bass and Braude, 'On the question of reflecting radar signals from the sun,' *Ukrainian Journal of Physics*, **2**, 149, 1957.
 17. Parrish, 'Solar Radar Experiments,' *Arecibo Observatory Internal Report*, CRSR 300, (D. Campbell, private communication), 1967.
 18. James, 'Radar studies of the sun,' in *Radar Astronomy*, edited by J. V. Evans and T. Hagfors, McGraw-Hill Book Company, New York, 1968.
 19. James, 'Some observed characteristics of solar radar echoes & their implications,' *Solar Physics*, **12**, 143-162, 1970.
 20. Rodriguez, P., 'Radar studies of the solar corona: A review of experiments using HF wavelengths,' in *Radio Astronomy at Long Wavelengths*, *Geophysics Monograph Series*, **119**, 155, 2000.
 21. Coles, W. A., J. K. Harmon, M. P. Sulzer, J. L. Chau, and R. F. Woodman, 'An upper bound on the solar radar cross section at 50 MHz,' *Journal of Geophysical Research*, **111**, A04102, doi: 10.1029/2005JA011416, 2006.
 22. Deller *et al.*, 'DiFX: A Software Correlator for Very Long Baseline Interferometry Using Multiprocessor Computing Environments,' *Publications of the Astronomical Society of the Pacific*, **119**, 318-336, 2007.
 23. Cohen *et al.*, 'The VLA Low-Frequency Sky Survey,' *Astronomical Journal*, **134**, 1245-1262, 2007.
 25. Perley and Bust, 'Probing the Ionosphere with the Very Large Array,' URSI General Assembly; 2002, [LWA Memo #8 \(http://www.ece.vt.edu/swe/lwa/memo/lwa0008.pdf\)](http://www.ece.vt.edu/swe/lwa/memo/lwa0008.pdf).
 25. Saha, 'Modern optical astronomy: technology and impact of interferometry,' *Reviews of Modern Physics*, **74**, 551-600, 200.
 26. Baldwin *et al.*, 'The first images from an optical aperture synthesis array: mapping of Capella with COAST at two epochs,' *Astronomy and Astrophysics*, **306L**, 13-16, 1996.
 27. Hummel *et al.*, 'First Observations with a Co-phased Six-Station Optical Long-Baseline Array: Application to the Triple Star η Virginis,' *Astronomical Journal*, **125**, 2630-2644, 2003.
 28. Cohen, 'A Potential Array Configuration for the LWA,' LWA Memo #55 (<http://www.ece.vt.edu/swe/lwa/memo/lwa0055a.pdf>), 2006.
 29. Cohen and Taylor, 'Array Configuration for the Long Wavelength Intermediate Array (LWIA),' LWA Memo #113 (<http://www.ece.vt.edu/swe/lwa/memo/lwa0113.pdf>), 2007.
 30. Taylor *et al.* 2009, LWA Memo #162 (<http://www.ece.vt.edu/swe/lwa/memo/lwa0162.pdf>)